Multiple-scattering theory for three-dimensional periodic acoustic composites

M. Kafesaki
Institute of Electronic Structure and Laser, Foundation for Research and Technology Hellas, P.O. Box 1527, 71110 Heraklion, Crete, Greece

E. N. Economou
Institute of Electronic Structure and Laser, Foundation for Research and Technology Hellas, P.O. Box 1527, 71110 Heraklion, Crete, Greece
and Department of Physics, University of Crete, Crete, Greece
(Received 17 May 1999)

We present results for acoustic wave propagation in periodic composites consisting of solid spheres in a fluid host. We show that for solid scatterers in fluid host material combinations the extensively used plane-wave method is inadequate to produce accurate results and a new approach is required. Our band-structure results are obtained by using a multiple-scattering approach based on an extension of the well-known Korringa-Kohn-Rostoker method. [S0163-1829(99)04841-9]

I. INTRODUCTION

The propagation of acoustic and elastic waves in periodic media is a problem of increasing interest in recent years. For the condensed matter physicists the interest is focused on the question of the existence or not of spectral gaps in these periodic media (phononic band gaps) in analogy with the electronic band gaps in metals or the photonic band gaps in photonic crystals. Materials with phononic band gaps (spectral regions where sound and vibrations are not permitted) can be proved very important for a lot of branches of science and technology: They can be used as sound filters, for the improvement of the design of transducers, as vibrationless environment for sensitive devices, etc. The interest for acoustic and elastic wave propagation stems also from the rich physics of the acoustic and elastic waves as well: the existence of a term proportional to the mass density variation in the acoustic and elastic wave equation or the mixed longitudinal and transverse vector character of the elastic waves are characteristics that distinguish them from other types of classical waves (waves obeying a second-order equation in the time domain). The investigation of the possible new features in the propagation coming from these particular characteristics is a challenging problem. Moreover, the acoustic and elastic composite media offer some important advantages (absence of interactions, precise tuning of the frequency) for the experimental investigation of questions related to localization—note that band gaps tend to be regions where localized states start to appear if we gradually disorder a periodic system.[1]

Based on the above considerations, several band-structure calculations for acoustic or elastic waves propagating in periodic composites consisting of spheres in a host material [three dimensional (3D)] or rods in a host material [two dimensional (2D)], where both the scatterers (spheres or rods) and the host are either fluids or solids appear.[2–12] Experimental studies were also performed[8,13–15] demonstrating the usefulness of acoustic waves in illustrating general features of wave propagation in inhomogeneous or random media. Most of the calculations have been performed using the plane-wave (PW) method. (In Ref. 8 a variational method was used based on an expansion in functions localized around each lattice point.) PW, which is based on the expansion of the periodic coefficients in the wave equation in Fourier sums, has been applied to a variety of realistic as well as ideal material combinations. Study within PW has shown that gaps can exist under rather extreme conditions that concern mainly the elastic parameters (density, velocities) of the components of the composite, the volume fraction of one of the two components, and the topology. More specifically, it has been found that the density contrast of the components of the composite plays a crucial role for the appearance of a gap. For solids, gaps are favored by high-density scatterers in a low-density host. In contrast, for fluids, low-density scatterers in a high-density host is the most favorable combination for gaps to appear.[4,5] Also gaps seem to prefer the cermet topology (isolated scatterers) rather than the network topology. Optimum (for gap formation) volume fraction of the scatterers ranges between 10–50 %. Ideal (for wide gap) realistic material combinations, according to the above conditions, can be composites consisting of heavy metal scatterers (e.g., Fe, steel, Pb) in a polymer host (e.g., epoxy).[6,9]

Although the existing theoretical study of 2D or 3D *fluid* or *solid* composites is quite extensive, this is not the case for *mixed* composites, i.e., composites consisting either of solid scatterers in a fluid host or of fluid scatterers in a solid host. The aim of this work is to study the case of *solid scatterers in a fluid host*. As we will show in the following, the PW is unable to give accurate results in this case. The attempts to find a method for the calculation of the band structure for solid scatterers in a fluid led us to extend to acoustic waves a variational multiple-scattering (MS) approach based on the well-known (in the band-structure electronic community) Korringa-Kohn-Rostoker (KKR) theory.[16–20] The success of this theory in the electronic band-structure calculations and, recently, in electromagnetic wave band-structure calculations,[21–23] combined with its ability to describe both fluid and solid scatterers and (most importantly) both peri-

odic and random media were the main reasons for our interest in the MS method. In the present work we apply the MS method in periodic composite systems consisting of spherical scatterers.

The structure of this paper is as follows: We will briefly present first PW, discussing its inability to describe composites with solid scatterers in a fluid. Then we will present our MS method, focusing also on the differences in the application of this method between the acoustic and the electronic case. Finally, we will present some of our main results. The results and some of our arguments will be discussed in connection with single-scattering data. It has been shown that single-scattering analysis, i.e., examination of the form of the single-scattering cross section, can give predictions and understanding for the band-structure characteristics (including the possible existence and the position of the gaps) in a periodic multiple-scattering system.[10,24,25] Usually, widely separated strong resonances in the cross section are combined to give flat bands in a periodic system, while gaps tend to appear between these flat bands.

II. ABOUT PW

PW is a fast and easy-to-apply method that is based on the expansion of the periodic coefficients in the wave equation and the periodic wave amplitude in Fourier series. Approximating these infinite Fourier series with finite sums, the solution of the wave equation is reduced to the solution of a finite matrix eigenvalue equation.

The elastic wave equation in isotropic systems has the following form:

$$\frac{1}{\rho}\left\{\frac{\partial}{\partial x_i}\left(\lambda\frac{\partial u^l}{\partial x_l}\right)+\frac{\partial}{\partial x_l}\left[\mu\left(\frac{\partial u^i}{\partial x_l}+\frac{\partial u^l}{\partial x_i}\right)\right]\right\}+\omega^2 u^i=0, \quad (1)$$

where u^i are the Cartesian components of the displacement vector, $\rho(\mathbf{r})$ is the mass density, and $\lambda(\mathbf{r})$ and $\mu(\mathbf{r})$ the Lamé coefficients of the medium [$\lambda=\rho(c_l^2-2c_t^2)$, $\mu=\rho c_t^2$, where c_l and c_t are the longitudinal and the transverse velocities, respectively]. For N terms in the Fourier sums ($\equiv N$ scatterers in the periodic medium) Eq. (1) leads to a $3N\times 3N$ eigenvalue equation, giving $3N$ permitted frequencies that correspond to mixed longitudinal and transverse waves.

For *fluid* systems $\mu=0$ and by introducing the pressure $p=-\lambda\nabla\mathbf{u}$, the above equation takes the form

$$\lambda(\mathbf{r})\nabla\left[\frac{1}{\rho(\mathbf{r})}\nabla p(\mathbf{r})\right]+\omega^2 p(\mathbf{r})=0. \quad (2)$$

Equation (2) is the starting point for the application of PW in fluid systems (fluid scatterers in a fluid host). For N terms in the Fourier sums one obtains in this case a $N\times N$ system.

Let us come now to the case of solid scatterers embedded in a fluid host. In that case the eigenmodes of the whole system (which are N for N scatterers) correspond to pure longitudinal waves. There are, however, transverse modes that cannot propagate, but they are localized inside the scatterers. (For a longitudinal wave incident on a scatterer, one can show that the field inside the scatterer will be both longitudinal and transverse.[26]) Due to the special, no propagating character of these modes, Eq. (1), with the application of PW, fails in the description of the propagation. Indeed, the attempts for such a calculation led to no convergence at all and unphysical solutions.

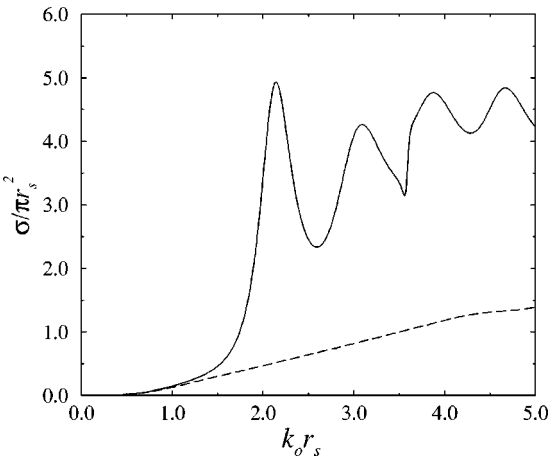

FIG. 1. Total dimensionless cross section ($\sigma/\pi r_s^2$) vs $k_o r_s=\omega r_s/c_o$ for a solid sphere in water (solid line) and for a fluid sphere of the same density and Lamé coefficient λ (dashed line) also embedded in water. r_s is the sphere radius.

On the other hand, one can obtain reasonable solutions using Eq. (2) (this is the method of some existing band-structure calculations[11]). Starting from Eq. (2), however, means that one ignores completely the difference of the wave equation inside the scatterers and, in fact, one replaces the solid scatterers with fluid scatterers (of the same λ and ρ) ignoring completely the transverse component of the wave within the scatterers. This transverse component, due to surface scattering, can be strongly coupled to the longitudinal component inside as well as outside the scatterers. Thus, we expect that it can considerably influence the longitudinal propagation modes in the entire system.

In order to obtain a first indication whether such an influence exists and to what extent, we examine first the single-scattering case. In Fig. 1 (solid line) we show the scattering cross section for a solid sphere with parameters $\rho_i=2.0$ g/cm^3, $c_{li}=3.0$ km/s, and $c_{ti}=1.5$ km/s, embedded in water. For the water $\rho_o=1.0$ g/cm^3, $c_{lo}=c_o=1.5$ km/s. [In the above and in what follows the subscript o (=out) denotes the host material and the subscript i (=in) the scattering material while the l and t denote longitudinal and transverse, respectively.] The dashed line in Fig. 1 shows the cross section for a fluid sphere of the same ρ and λ as the solid one [$\rho=\rho_i$, $\lambda=\rho_i(c_{li}^2-2c_{ti}^2)$], embedded also in water. As it is clear from Fig. 1, the substitution of a solid sphere by a fluid one of the same ρ and λ [what PW with Eq. (2) does] produces huge changes in the cross section. This, combined with our experience of the strong connection between the single-scattering cross section and the band structure, is an indication that we can expect considerable difference also in the band structure. Thus, the band-structure results provided by the combination of Eq. (2) and the PW method can be very inaccurate. The confirmation of this last statement will come from the comparison of the PW result with the result of the MS method, which we present next. The MS method takes into account the exact character of the problem and it can be also applied to the full fluid case (fluid scatterers and host) with limited additional effort.

III. MULTIPLE-SCATTERING (MS) METHOD

As has been already mentioned, our multiple-scattering method is based on the KKR theory. We start from the acoustic wave equation in a periodic medium, Eq. (2). An alternative way to write this equation is

$$\nabla^2 p(\mathbf{r}) + \frac{\omega^2}{c_o} p(\mathbf{r}) + \omega^2 \left[\frac{1}{c^2(\mathbf{r})} - \frac{1}{c_o^2} \right] p(\mathbf{r}) + \rho(\mathbf{r}) \times \left[\nabla \frac{1}{\rho(\mathbf{r})} \right] \nabla p(\mathbf{r}) = 0. \tag{3}$$

Equation (3) has the form

$$H_0(\mathbf{r}) p(\mathbf{r}) + U(\mathbf{r}) p(\mathbf{r}) = 0, \tag{4}$$

where $H_0(\mathbf{r}) p(\mathbf{r}) = 0$ $[H_0(\mathbf{r}) = \nabla^2 + \omega^2 / {c_o}^2]$ represents the wave equation in the absence of scatterers (c_o is the wave velocity in the host material). Equation (4) has the same form as the Schrödinger equation for the electron waves. This analogy indicates that one can apply the KKR theory in a similar way as in the electronic case. There is, however, an important difference between our case and the electronic case. The difference stems from the fact that the potential in our case has a δ-function singularity at the surface of the scatterers due to the factor $\nabla \rho^{-1}$. Thus, the contribution of the surface scattering to the volume integrals is not negligible (as in the electronic case[17]). Due to this difference we will present our calculations in some detail despite the fact that analogous calculations have been presented in the literature for the electronic case.[17,20,18]

It can be easily shown[20] that in a periodic system Eq. (3) is equivalent to the following integral equation:

$$p(\mathbf{r}) = \int_v G(\mathbf{r}-\mathbf{r}') V(\mathbf{r}') p(\mathbf{r}') d\mathbf{r}', \tag{5}$$

where v is the volume of a unit shell and the function $G(\mathbf{r}-\mathbf{r}')$ is given by

$$G(\mathbf{r}-\mathbf{r}') = \sum_n e^{i\mathbf{k}\cdot\mathbf{R}_n} G_0(\mathbf{r}-\mathbf{r}'-\mathbf{R}_n). \tag{6}$$

G_0 is the Green's function[27] for the homogeneous equation $H_0(\mathbf{r}) p(\mathbf{r}) = 0$:

$$G_0(\mathbf{r}-\mathbf{r}') = -\frac{1}{4\pi} \frac{e^{ik_o|\mathbf{r}-\mathbf{r}'|}}{|\mathbf{r}-\mathbf{r}'|}, \quad k_o = \frac{\omega}{c_o}. \tag{7}$$

The local potential $V(\mathbf{r})$ in Eq. (5) is zero outside the unit shell centered at the origin of the coordinate system [it is related to U by $U(\mathbf{r}) = \Sigma_n V(\mathbf{r}-\mathbf{R}_n)$], and the pressure field, $p(\mathbf{r})$, obeys the Bloch's condition, $p(\mathbf{r}+\mathbf{R}_n) = \exp(i\mathbf{k}\cdot\mathbf{R}_n) p(\mathbf{r})$.

Taking into account that for acoustic waves the local potentials V are nonzero only inside and at the surface of the scatterers [see Eq. (3)], the integral over the unit shell in Eq. (5) is reduced to an integral over the volume of a scatterer ($r' \leqslant r_s$, r_s is the scatterer radius):

$$\int_v d\mathbf{r}' = \lim_{\epsilon \to 0+} \int_{r' \leqslant r_s + \epsilon} d\mathbf{r}'. \tag{8}$$

The limiting procedure in Eq. (8) ensures that we approach the surface of the sphere from the outside, including thus the surface singularity.

By noticing that for nonoverlapping spheres and $\mathbf{r}$, $\mathbf{r}'$ inside a unit shell centered at the origin of the coordinate system the function G obeys the equation

$$\nabla^2 G(\mathbf{r}-\mathbf{r}') + k_o^2 G(\mathbf{r}-\mathbf{r}') = \delta(\mathbf{r}-\mathbf{r}'), \tag{9}$$

and by using the wave equation and the Gauss theorem, the volume integral in Eq. (8) can be transformed to a surface integral. After some algebraic manipulations one can find that

$$\lim_{r' \to r_s +} \int_{S'} [p(\mathbf{r}') \nabla_{r'} G(\mathbf{r}-\mathbf{r}') - G(\mathbf{r}-\mathbf{r}') \nabla_{r'} p(\mathbf{r}')] d\mathbf{S}' = \begin{cases} p(\mathbf{r}) & \text{for } r > r_s \\ 0 & \text{for } r < r_s, \end{cases} \tag{10}$$

where S' is a spherical surface of radius r', centered at the origin of the coordinates.

The $r' \to r_s +$ in the above limit denotes that we approach the sphere surface from the outside. This is a direct consequence of Eq. (8) and it is very important in our case as the integrated functions are not continuous across the surface (the pressure is continuous but its derivative has a step function discontinuity) and thus the side limits do not coincide. This discontinuity of the integrated functions does not occur in the electron wave case, where the usual practice is to consider the above integral as an ''inwards'' integral ($r' \to r_s -$).[17,20]

The solution of Eq. (10) for $r < r_s$ gives the eigenfrequencies of our periodic system for each Bloch's vector $\mathbf{k}$. To obtain this solution we use the fact that both the functions $G(\mathbf{r}-\mathbf{r}')$ and $p(\mathbf{r}')$ can be expanded in spherical functions of $\mathbf{r}$ and $\mathbf{r}'$ (see Appendix B):

$$G(\mathbf{r}-\mathbf{r}') = \sum_{lm} \sum_{l'm'} [A_{lml'm'} j_l(k_o r) j_{l'}(k_o r') + k_o j_l(k_o r) y_{l'}(k_o r') \delta_{ll'} \delta_{mm'}] \times Y_{lm}(\mathbf{r}) Y^*_{l'm'}(\mathbf{r}') \quad (\text{for } r < r'), \tag{11}$$

$$p(\mathbf{r}')|_{r' \geqslant r_s} = p^{out}(\mathbf{r}') = \sum_{lm} a_{lm} [j_l(k_o r') + t_l h_l(k_o r')] Y_{lm}(\mathbf{r}'). \tag{12}$$

(In the above equations j_l and y_l are the first- and second-kind spherical Bessel functions of order l and $h_l = j_l + i y_l$.)

Substituting Eq. (11) and Eq. (12) into Eq. (10) we obtain the final multiple-scattering equation:

$$\sum_{l'm'} [A_{lml'm'} - k_o \mathrm{Im}(t_{l'}^{-1}) \delta_{ll'} \delta_{mm'}] a_{l'm'} = 0. \tag{13}$$

The coefficients $A_{lml'm'}$ in the above equations are called structure constants and they depend on $\mathbf{k}$, ω, and the lattice structure. Their calculation is described in Appendix B. The coefficients t_l, relating the incident to the scattered field at each scatterer, can be calculated by solving a single-scattering problem (see Appendix D).

Equation (13) can be written as

$$\sum_{l'm'} \Lambda_{lml'm'} a_{l'm'} = 0 \Leftrightarrow \sum_{L'} \Lambda_{LL'} a_{L'} = 0, \quad L \equiv (l,m), \tag{14}$$

which corresponds to a linear homogeneous algebraic system. The condition for this system to have nonvanishing solutions, $\det(\Lambda)=0$, gives the eigenfrequencies of our periodic composite.

A careful examination of the above equations shows that the elastic parameters of the scattering material affect the calculation only through the scattering coefficients t_l. t_l can be calculated very easily and accurately for both solid and fluid scatterers. Thus, the method can be applied to both solid and fluid scatterers changing only the form of a single-scattering problem. This, however, is not the only advantage of the method. Its most important advantage, as has been already mentioned, is that it can be applied also in disordered systems. It can treat systems with positional as well as substitutional disorder [the latter can be done by combining the KKR method with the coherent potential approximation (CPA) method].

An alternative way to obtain Eq. (14) is to convert the ''outwards'' integral (10) to an ''inwards'' integral and to use the pressure field inside a sphere. (This is the way that the KKR has been applied in the electronic case, but there the distinction between ''inwards'' and ''outwards'' integral does not matter as the two integrals coincide.) The conversion to an ''inwards'' integral (for fluid scatterers) can be done by taking into account the boundary conditions of the acoustic scattering problem,

$$\lim_{r' \to r_s +} p(r') = \lim_{r' \to r_s -} p(r'),$$

$$\lim_{r' \to r_s +} \frac{\partial}{\partial r'} p(r') = \lim_{r' \to r_s -} \frac{\rho_o}{\rho_i} \frac{\partial}{\partial r'} p(r'). \tag{15}$$

With the boundary conditions (15), the integral (10) (for $r<r_s$, $r<r'$) becomes

$$\lim_{r' \to r_s -} \int_{S'} \left[\rho_i p(\mathbf{r}') \frac{\partial}{\partial r'} G(\mathbf{r}-\mathbf{r}') - \rho_o G(\mathbf{r}-\mathbf{r}') \frac{\partial}{\partial r'} p(\mathbf{r}') \right] d\mathbf{S}_n' = 0 \tag{16}$$

and Eq. (14) can be obtained by substituting in this integral the expansion of the function G [see Eq. (11)], the pressure field inside a scatterer,

$$p^{in}(\mathbf{r}) = \sum_{lm} d_{lm} j_l(k_i r) Y_{lm}(\mathbf{r}), \quad k_i = \frac{\omega}{c_i}, \tag{17}$$

and by taking into account the form of t_l [see Eq. (D1)]. (c_i is the wave velocity inside the scatterers.) For solid scatterers the conversion of (10) to an ''inwards'' integral is a more complicated problem.

A. Calculational details

As we discussed above, the eigenmodes of a periodic system are obtained by requiring nonvanishing solutions for the linear homogeneous system (14). Thus, one has to calculate the matrix Λ, the determinant of which has to be set equal to zero [see Eq. (14)]. The order of the matrix Λ depends on the number of the angular momentum terms that we keep in the field function (12) [or (17)]. In our calculations we obtained good convergence by keeping the maximum number of $l = l_{max} = 3$ or 4, while for the lower bands we had good convergence with l_{max} less than 3.

Another parameter of the problem is the size of the periodic system. In the results shown in this paper we have considered a system of 400–500 lattice vectors in the direct as well as the reciprocal lattice, with excellent convergence.

The solution of the secular equation (14) by checking the vanishing of the determinant through its sign change involves the risk of losing some multiple solutions. One way to face this difficulty is to diagonalize Λ first and then find the sign changes of each of the resulting diagonal elements (which have no multiple roots).

Among the calculational problems of the MS method one worth mentioning is the problem of the spurious ''roots'' (sign changes of the determinant that do not correspond to actual eigenfrequencies of the system). We met these kinds of roots in two cases: (a) For $k_o = \omega/c_o \approx |\mathbf{k}+\mathbf{G}_n|$ ($\mathbf{G}_n$ is any vector of the reciprocal lattice). For these values of k_o the structure constants $A_{lml'm'}$ become singular (see Appendixes B and C) and there is a possibility that the determinant or an eigenvalue of Λ may change sign without the existence of a real eigenfrequency of the system. (For actual eigenfrequencies one or more eigenvalues of Λ have to approach zero continuously as we approach the eigenfrequency.) For the calculation of eigenmodes of the system with $k_o = \omega/c_o \approx |\mathbf{k}+\mathbf{G}_n|$ the MS method is a bit inconvenient. (b) We met spurious roots also for frequencies for which the coefficient t_l becomes zero. The actual eigenmodes of the system close to these frequencies, if they exist, can be found if one replaces the Λ by its submatrix which arises by subtracting the rows and the columns corresponding to the l for which $t_l = 0$.[19]

IV. RESULTS AND DISCUSSION

In what follows we present some of our main results. One of our aims is to examine how important is the nonvanishing rigidity of the scatterers for the band structure. For that reason we compare our reliable MS results with results obtained within PW or, equivalently, with band-structure results for corresponding fluid scatterers (fluid scatterers with the same λ and ρ as the solid ones).

Our first result (see Fig. 2) concerns the material combinations of Fig. 1. Figure 2(a) shows the band structure along the $L\Gamma$ and ΓX directions for an fcc periodic composite consisting of solid spheres (with the same parameters as in Fig.

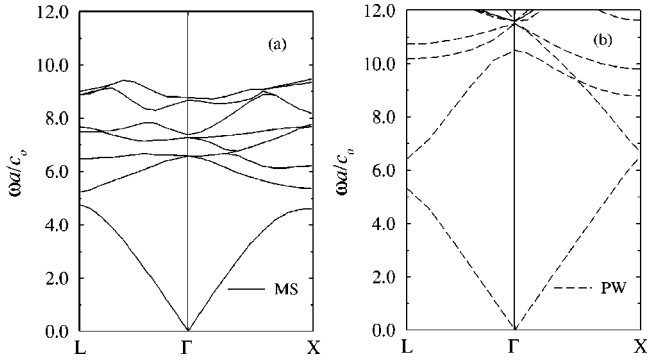

FIG. 2. Dispersion relation along the $L\Gamma$ and ΓX directions for an fcc periodic composite consisting of solid spheres in water. The parameters are as follows: $\rho_o/\rho_i=1/2$, $c_o/c_{li}=1/2$, $\lambda_o/\lambda_i=1/4$, $c_{ti}/c_{li}=1/2$. Volume fractions of spheres $f=50\%$. c_o is the wave velocity in the host and a the lattice constant. (a) shows the result within MS method and (b) the same within PW and Eq. (2).

1) in water host. The volume fraction of the spheres is $f_s=50\%$. Figure 2(b) shows the band structure for fluid spheres of the same λ and ρ as the solid ones and in the same periodic arrangement, also in water host. Figure 2(b) is what PW [with Eq. (2)] gives for the material combination of Fig. 2(a). As can be seen the PW results are very different from those of the MS method. This difference shows that the replacement of the solid scatterers with fluids can change the band structure drastically.

A realistic case similar to the previous one is presented in Fig. 3. Figure 3 shows the band structure for a system consisting of glass spheres in water, in sc structure and glass volume fraction $f=45\%$. (For glass $\rho=2.5$ g/cm^3, $c_l=5.7$ km/s, $c_t=3.4$ km/s.) Again, here, the left panel is our MS method result and the right one is what the combination of Eq. (2) and PW provides in this case, i.e., the band structure for fluid spheres of the same λ and ρ as in glass.

As can be seen in Fig. 3, the difference between the MS and the PW result is reduced compared to the previous case (Fig. 2). This reduction can been predicted by calculating the cross section for a glass sphere embedded in water and the cross section of a fluid sphere of the same λ and ρ as in the glass embedded also in water (see Fig. 4). The difference

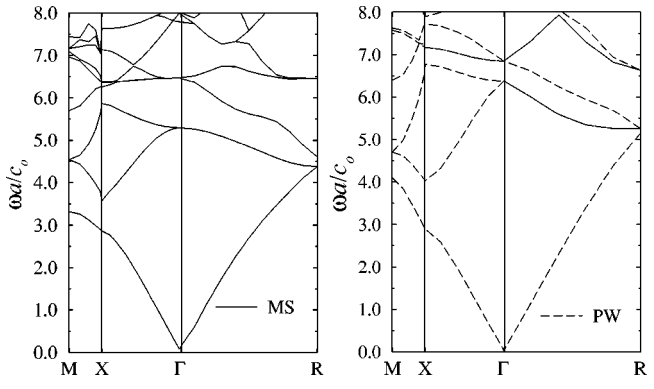

FIG. 3. Dispersion relation along the $MX\Gamma R$ directions for a sc periodic composite consisting of glass spheres in water. Glass volume fraction $f=45\%$. c_o is the wave velocity in the water and a the lattice constant.

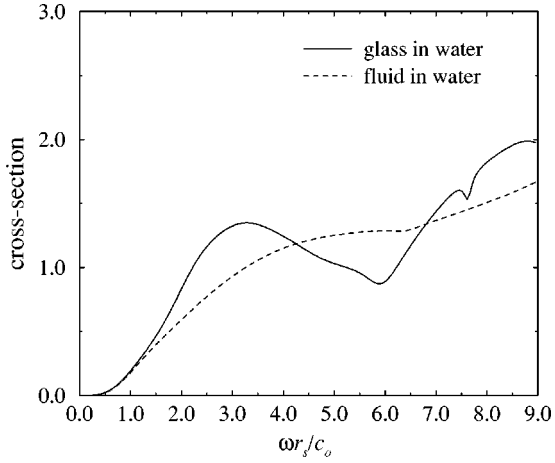

FIG. 4. Solid line: single-scattering cross section $\sigma/\pi r_s^2$ for a glass sphere in water host. Dashed line: single-scattering cross section for a fluid sphere with the ρ and λ as in the glass, also embedded in water. c_o is the wave velocity in the water and r_s the sphere radius.

between the two curves is considerably less than the difference between the solid and dashed line in Fig. 1.

The reduction of the difference between the PW and the MS result in the case described in Fig. 3 compared to that of Fig. 2, which actually means reduction of the influence of the rigidity of the scatterers, can be attributed to the larger velocity and density contrast between scatterers and host. As has been discussed in the past[5,24] the velocity and mainly the density contrast between scatterers and host are the most important parameters controlling the scattering and thus the propagation in the composite system. As these contrasts increase, other parameters, as the rigidity of the scatterers, become less important.

To demonstrate this point we examine the case of steel spheres in air. The band structure obtained by the MS method (see Fig. 5, circles) is the same as that obtained for fluid spheres with the λ and ρ as in steel (see Fig. 5, solid line). The origin of this coincidence comes from the extremely large density contrast between steel and air. This

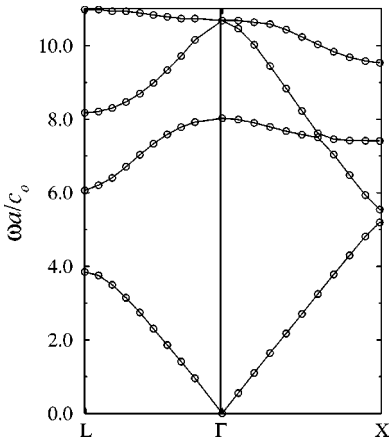

FIG. 5. Dispersion relation along the $L\Gamma X$ directions for a fcc periodic composite consisting of steel spheres in air (steel volume fraction $f=65\%$). The circles indicate our MS result and the solid line the corresponding PW result. c_o is the wave velocity in the air and a the lattice constant.

large density contrast is the dominant parameter for the scattering and, consequently, for the band structure. Thus, the existence of a nonvanishing shear velocity in the spheres does not play a significant role. We can also understand it by taking into account that a steel sphere in air is almost equivalent to a ''hard'' (inpenetrable) sphere, which permits no wave to get in. Thus, the details of wave propagation inside the sphere are irrelevant.

An examination of material combinations other than these shown in Figs. 2, 3, and 5 leads to the result that the role of the scatterer shear velocity or μ becomes important for the band structure only when both the density and the longitudinal velocity contrast between scatterers and host are relatively low. When either the velocity or the density contrast starts to get higher, the role of the scatterers c_t (or μ) becomes less and less important. The most extreme case is that of high-density contrast, where the shear velocity in the scatterers does not seem to affect the band structure at all. This last case is the one that the PW method can describe very accurately.[11]

V. CONCLUSIONS

In this work we extended the multiple-scattering KKR method and we presented band-structure results for acoustic waves propagating in periodic composites consisting of solid spherical scatterers in a fluid host. We calculated the band structure for a variety of material combinations and we examined whether and under what conditions the scatterer shear velocity affects the propagation. For this purpose we compared the MS-KKR results with those based on the PW method, which calculates the band structure approximating the solid scatterers with fluid ones. We found that the scatterer's shear velocity is important for the determination of the band structure only in the case of low-density and low-velocity contrast between scatterers and host.

ACKNOWLEDGMENTS

We would like to thank Dr. Xindong Wang for useful communications. Thanks also are due to Dr. M. Sigalas for providing us with his PW band-structure programs. This work was supported by European Union and Greek Government grants.

APPENDIX A: TRANSFORMATIONS OF FUNCTIONS; ELEMENTARY FUNCTIONS; USEFUL EXPANSIONS

1. Expansion of a plane wave

$$e^{i\mathbf{k}\cdot\mathbf{r}}=4\pi\sum_{lm} i^l j_l(kr)Y_{lm}(\mathbf{r})Y^*_{lm}(\mathbf{k}), \tag{A1}$$

where the spherical harmonics $Y_{lm}(\mathbf{r})$ are given by

$$Y_{lm}(\mathbf{r})=Y_{lm}(\hat{\mathbf{r}})=\left[\frac{2l+1}{4\pi}\frac{(l-|m|)!}{(l+|m|)!}\right]^{1/2}P_l^{|m|}(\cos\theta)e^{im\phi},$$

$$\mathbf{r}=(r,\theta,\phi), \quad m\geqslant 0 \tag{A2}$$

and

$$Y_{l-m}(\hat{\mathbf{r}})=(-1)^m Y^*_{lm}(\hat{\mathbf{r}}), \quad Y_{lm}(-\hat{\mathbf{r}})=(-1)^l Y_{lm}(\hat{\mathbf{r}}). \tag{A3}$$

2. Transformations of elementary spherical functions

$$h_l(k|\mathbf{r}-\mathbf{r}'|)Y_{lm}(\mathbf{r}-\mathbf{r}')=\begin{cases}\displaystyle\sum_{l'm'} j_{l'}(kr)Y_{l'm'}(\mathbf{r})g^{(h)}_{l'm'lm}(\mathbf{r}') & \text{for } r<r'\\ \displaystyle\sum_{l'm'} h_{l'}(kr)Y_{l'm'}(\mathbf{r})g^{(j)}_{l'm'lm}(\mathbf{r}') & \text{for } r>r',\end{cases} \tag{A4}$$

where

$$g^{(R)}_{l'm'lm}(\mathbf{D})=\sum_{LM}(-1)^{(l'-l-L)/2}4\pi C_{l'm'lmLM}\times R_L(kD)Y_{LM}(\mathbf{D}), \quad R=j \text{ or } h. \tag{A5}$$

$C_{l'm'lmLM}$ are the Gaunt numbers:[28]

$$C_{l'm'lmLM}=\int Y_{l'm'}(\mathbf{r})Y^*_{lm}(\mathbf{r})Y_{LM}(\mathbf{r})d\Omega_{\mathbf{r}} \tag{A6}$$

$$=\frac{(-1)^m}{\sqrt{4\pi}}[(2l+1)(2l'+1)(2L+1)]^{1/2}\times\begin{pmatrix}l' & l & L\\ 0 & 0 & 0\end{pmatrix}\begin{pmatrix}l' & l & L\\ m' & -m & M\end{pmatrix}.$$

The symbols with the parentheses are the $3j$ symbols.[28] For given l,m,l',m' the only value of M that gives nonzero $C_{l'm'lmLM}$ is $M=m-m'$. Thus, the double sum in Eq. (A5) is in fact a sum only over L, with $M=m-m'$.

According to the above,

$$-\frac{1}{4\pi}\frac{e^{ik|\mathbf{r}-\mathbf{r}'|}}{|\mathbf{r}-\mathbf{r}'|}=-i\frac{k}{\sqrt{4\pi}}h_0(k_o|\mathbf{r}-\mathbf{r}'|)Y_{00}(\mathbf{r}-\mathbf{r}')$$

$$=-ik\sum_{lm} j_l(kr)Y_{lm}(\mathbf{r})h_l(kr')\times Y^*_{lm}(\mathbf{r}'), \quad r<r'. \tag{A7}$$

The regular spherical function $j_l(k|\mathbf{r}-\mathbf{r}'|)Y_{lm}(\mathbf{r}-\mathbf{r}')$ can be transformed[17] as

$$j_l(k|\mathbf{r}-\mathbf{r}'|)Y_{lm}(\mathbf{r}-\mathbf{r}')=\frac{1}{4\pi i^l}\int e^{i\mathbf{k}\cdot(\mathbf{r}-\mathbf{r}')}Y_{lm}(\mathbf{k})d\Omega_{\mathbf{k}}$$

$$=\sum_{l'm'} j_{l'}(kr)Y_{l'm'}(\mathbf{r})g^{(j)}_{l'm'lm}(\mathbf{r}'). \tag{A8}$$

From Eq. (A4) and Eq. (A8) it can also be seen that

$$-\frac{1}{4\pi}\frac{\cos(k|\mathbf{r}-\mathbf{r}'|)}{|\mathbf{r}-\mathbf{r}'|}$$

$$=k\sum_{lm} j_l(kr)Y_{lm}(\mathbf{r})y_l(kr')Y^*_{lm}(\mathbf{r}'), \quad r<r'. \tag{A9}$$

APPENDIX B: THE STRUCTURE CONSTANTS $A_{lml'm'}$

Starting from the expression of the free space Green's function, G_0 [Eq. (7)], and using Eq. (6) and the formulas of Appendix A, we can express the function $G(\mathbf{r}-\mathbf{r}')=G(\mathbf{r}'')$ (with $r''<|\mathbf{R}_n|$ for each $\mathbf{R}_n\neq 0$) as[17]

$$G(\mathbf{r}'')=\sum_{\mathbf{R}_n} e^{i\mathbf{k}\cdot\mathbf{R}_n}G_0(\mathbf{r}''-\mathbf{R}_n)$$

$$=\sum_{LM} D_{LM}\, j_L(k_o r'')Y_{LM}(\mathbf{r}'')-\frac{1}{4\pi}\frac{\cos(k_o r'')}{r''}, \tag{B1}$$

where

$$D_{LM}=-ik_o\left[\sum_{\mathbf{R}_n\neq 0} e^{i\mathbf{k}\cdot\mathbf{R}_n}h_L(k_oR_n)Y^*_{LM}(\mathbf{R}_n)+\frac{1}{4\pi}\delta_{L0}\delta_{M0}\right]. \tag{B2}$$

Expanding the functions $j_L(k_o r'')Y_{LM}(\mathbf{r}'')$ and $\cos(k_o''r)/r''$ according to Eq. (A8) and Eq. (A9) and comparing with Eq. (11), we can express $A_{lml'm'}$ as

$$A_{lml'm'}=\sum_{LM} 4\pi i^{l-l'-L}C_{l'm'lmLM}D_{LM}. \tag{B3}$$

Thus, the structure constants $A_{lml'm'}$ can be calculated through D_{LM}. The calculation of D_{LM} requires calculation of a sum over all lattice sites. In order to ensure the convergence of this sum a usual practice is the application of Ewald's summation[29] (see Appendix C).

APPENDIX C: CALCULATION OF THE SUMS—EWALD'S SUMMATION

Ewald's summation has been applied in the literature[18] to the sum contained in the function $G(\mathbf{r}-\mathbf{r}')=G(\mathbf{r}'')$ [see Eq. (6)]. Using the integral representation of the Hankel function h_0, G can be written as

$$G(\mathbf{r}'')=\frac{-ik_o}{4\pi}\sum_{\mathbf{R}_n} e^{i\mathbf{k}\cdot\mathbf{R}_n}h_0(k_o|\mathbf{r}''-\mathbf{R}_n|) \tag{C1}$$

$$=\frac{-1}{2\pi\sqrt{\pi}}\sum_{\mathbf{R}_n} e^{i\mathbf{k}\cdot\mathbf{R}_n}\int_0^\infty e^{-(\mathbf{r}''-\mathbf{R}_n)^2\xi^2+k_o^2/4\xi^2}d\xi \tag{C2}$$

$$=\frac{-1}{2\pi\sqrt{\pi}}\sum_{\mathbf{R}_n} e^{i\mathbf{k}\cdot\mathbf{R}_n}$$

$$\times\left[\int_0^{\sqrt{\eta/2}}d\xi+\int_{\sqrt{\eta}/2}^\infty d\xi\right]e^{-(\mathbf{r}''-\mathbf{R}_n)^2\xi^2+k_o^2/4\xi^2}, \tag{C3}$$

where η is a positive number. Applying Ewald's condition,[29]

$$\sum_{\mathbf{R}_n} e^{-(\mathbf{r}-\mathbf{R}_n)^2\xi^2+i\mathbf{k}\cdot(\mathbf{R}_n-\mathbf{r})}=\frac{\pi\sqrt{\pi}}{v\xi^3}\sum_{\mathbf{G}_n} e^{-(\mathbf{k}+\mathbf{G}_n)^2/4\xi^2+i\mathbf{G}_n\cdot\mathbf{r}}, \tag{C4}$$

to the first integral in Eq. (C3) and comparing the result with Eq. (B1) in the limit $r''\to 0$, one can obtain the following expressions for the coefficients D_{LM}:

$$D_{LM}=D^{(1)}_{LM}+D^{(2)}_{LM}+D^{(3)}_{00}\delta_{L0}\delta_{M0}, \tag{C5}$$

$$D^{(1)}_{LM}=-\frac{1}{v}\sum_{\mathbf{G}_n}\frac{4\pi i^L}{(\mathbf{k}+\mathbf{G}_n)^2-k_o^2}$$

$$\times e^{[-(\mathbf{k}+\mathbf{G}_n)^2+k_o^2]/\eta}\frac{|\mathbf{k}+\mathbf{G}_n|^L}{k_o^L}Y^*_{LM}(\mathbf{k}+\mathbf{G}_n), \tag{C6}$$

$$D^{(2)}_{LM}=-\frac{2^{L+1}}{k_o^L\sqrt{\pi}}\sum_{\mathbf{R}_n\neq 0} R_n^L e^{i\mathbf{k}\cdot\mathbf{R}_n}Y^*_{LM}(\mathbf{R}_n)$$

$$\times\int_{\sqrt{\eta}/2}^\infty \xi^{2L}e^{-R_n^2\xi^2+k_o^2/4\xi^2}d\xi, \tag{C7}$$

$$D^{(3)}_{00}=-i^L\frac{\sqrt{\eta}}{2\pi}\sum_{s=0}^\infty\frac{(k_o^2/\eta)^s}{s!(2s-1)}. \tag{C8}$$

(The i^L difference between our expressions for the D_{LM}'s and the corresponding expressions of Ref. 18 is due to the difference in the definition of the D_{LM}.)

The structure constants $A_{lml'm'}$ are calculated combining the above expressions for D_{LM} with Eq. (B3). The convergence of the sums in $D^{(1)}_{LM}$ and $D^{(2)}_{LM}$ depends on the choice of the parameter η. Usually a good choice is a value that makes $D^{(1)}_{LM}$ of the same order with $D^{(2)}_{LM}$.

From the above it means that the calculation of the sum

$$Z_{LM}(\mathbf{k})=\sum_{\mathbf{R}_n\neq 0} e^{i\mathbf{k}\cdot\mathbf{R}_n}h_L(k_oR_n)Y^*_{LM}(\mathbf{R}_n) \tag{C9}$$

according to Ewald's procedure is done through the expression $\Sigma_{LM}j_L(k_or)Y_{LM}(\mathbf{r})Z_{LM}(\mathbf{k})$. Taking into account that

$$\sum_{LM} j_L(k_or)Y_{LM}(\mathbf{r})Z_{LM}(\mathbf{k})+\frac{1}{\sqrt{4\pi}}h_0(k_or)Y_{00}(\mathbf{r})$$

$$=\frac{-i}{k_o}\frac{1}{4\pi}\sum_{\mathbf{R}_n} e^{i\mathbf{k}\cdot\mathbf{R}_n}\frac{e^{ik_o|\mathbf{r}-\mathbf{R}_n|}}{|\mathbf{r}-\mathbf{R}_n|}, \tag{C10}$$

and transforming the right-hand side according to Ewald's procedure in the limit $r\to 0$, one can obtain the Ewald's expression for Z_{LM}. Also,

$$H_{LM}(\mathbf{k})=\sum_{\mathbf{R}_n\neq 0} e^{-i\mathbf{k}\cdot\mathbf{R}_n}h_L(k_oR_n)Y_{LM}(\mathbf{R}_n)$$

$$=(-1)^{L+M}Z_{L-M}(\mathbf{k}). \tag{C11}$$

APPENDIX D: CALCULATION OF THE SCATTERING COEFFICIENTS t_n

The coefficient t_n connects the scattered to the incident field at each scatterer. (To avoid the confusion between the subscript that denotes the spherical harmonic and the subscript that denotes ''longitudinal,'' in this appendix we will denote the first with n.) For a fluid scatterer in a fluid host it can be calculated by considering the pressure fields (12) and (17) and applying the boundary conditions (15). The resulting expression is

$$t_n=\frac{-(k_o/\rho_o)j_n(k_ir_s)j_n'(k_or_s)+(k_i/\rho_i)j_n'(k_ir_s)j_n(k_or_s)}{(k_o/\rho_o)j_n(k_ir_s)h_n'(k_or_s)-(k_i/\rho_i)j_n'(k_ir_s)h_n(k_or_s)}$$
$$=\frac{1}{-1+iw_n},\quad w_n=\mathrm{Im}(t_n^{-1})=\text{real}. \tag{D1}$$

For a solid scatterer in a fluid host the boundary conditions at the surface of the scatterer require continuity of the normal component of the displacement vector $\mathbf{u}$, continuity of the normal component of the stress vector, and vanishing of the tangential component of the stress vector.[24,26] Taking into account that in a homogeneous medium $\mathbf{u}(\mathbf{r})=(1/\rho\omega)\nabla p(\mathbf{r})$, one can calculate the incident displacement vector for a given pressure field. Applying, then, the above mentioned boundary conditions, t_n can be calculated as follows:

$$t_n=\frac{1}{D_n}\begin{vmatrix} a_{14} & a_{12} & a_{13}\\ a_{24} & a_{22} & a_{23}\\ a_{34} & a_{32} & a_{33}\end{vmatrix}=\frac{1}{-1+iv_n},$$

$$D_n=\begin{vmatrix} a_{11} & a_{12} & a_{13}\\ a_{21} & a_{22} & a_{23}\\ a_{31} & a_{32} & a_{33}\end{vmatrix},\quad v_n=\mathrm{Im}(t_n^{-1}); \tag{D2}$$

$$a_{11}=h_n'(Z_o),\quad a_{12}=-j_n'(Z_{li}),$$

$$a_{13}=-n(n+1)j_n(Z_{ti})/Z_{ti},\quad a_{14}=-j_n'(Z_o); \tag{D3}$$

$$a_{21}=Z_o[-\lambda_o h_n(Z_o)],$$

$$a_{22}=-Z_{li}[2\mu_i j_n''(Z_{li})-\lambda_i j_n(Z_{li})],$$

$$a_{23}=-2n(n+1)\mu_i[j_n'(Z_{ti})-j_n(Z_{ti})/Z_{ti}],$$

$$a_{24}=Z_o[\lambda_o j_n(Z_o)]; \tag{D4}$$

$$a_{31}=a_{34}=0,\quad a_{32}=-2\mu_i[j_n'(Z_{li})-j_n(Z_{li})/Z_{li}],$$

$$a_{33}=-\mu_i[Z_{ti}j_n''(Z_{ti})+(n-1)(n+2)j_n(Z_{ti})/Z_{ti}]. \tag{D5}$$

In the above equations $Z_o=\omega r_s/c_o$, $Z_{li}=\omega r_s/c_{li}$, $Z_{ti}=\omega r_s/c_{ti}$, and r_s is the sphere radius.

APPENDIX E: SIMPLE MULTIPLE-SCATTERING FORMALISM

In the following we will show that we can obtain the multiple-scattering secular equation (14) without the use of the integral equation (10) and using only a physical multiple-scattering picture. This picture is based on the simple idea that in a multiple-scattering system (either periodic or random) the incident wave at each scatterer n, p_n^{inc}, has to be equal to the sum of the scattered waves from all the other scatterers, plus, possibly, an external field p^0 incident to the composite system.[16] This idea can be expressed mathematically as follows:

$$p_n^{inc}(\mathbf{r})=p^0(\mathbf{r})+\sum_{p\neq n}p_p^{sc}(\mathbf{r}), \tag{E1}$$

where the subscript n denotes the scatterer at the lattice position $\mathbf{R}_n$. We can write the incident and the scattered wave at each lattice position as a sum of elementary spherical waves:

$$p_n^{inc}(\mathbf{r})=p^{inc}(\mathbf{r}-\mathbf{R}_n)=\sum_{lm}a_{lm}^n j_l(k_o|\mathbf{r}-\mathbf{R}_n|)Y_{lm}(\mathbf{r}-\mathbf{R}_n), \tag{E2}$$

$$p_n^{sc}(\mathbf{r})=p^{sc}(\mathbf{r}-\mathbf{R}_n)=\sum_{lm}b_{lm}^n h_l(k_o|\mathbf{r}-\mathbf{R}_n|)Y_{lm}(\mathbf{r}-\mathbf{R}_n). \tag{E3}$$

Relating the scattered wave by each scatterer with the incident wave at the same scatterer by solving a simple single-scattering problem (see Appendix D), one can relate the coefficients b_{lm}^n with the a_{lm}^n:

$$b_{lm}^n=t_l a_{lm}^n. \tag{E4}$$

The scattering coefficients t_l [see Eq. (D1) and Eq. (D2)] are independent of the lattice position n only in the case of identical scatterers.

We are interested for the eigenfrequencies of the system, which means solutions with external field equal to zero. Setting $p^0(\mathbf{r})=0$ in Eq. (E1), using Eqs. (E2), (E3), and (E4), and the expansions of the elementary spherical functions $h_l(k_o|\mathbf{r}-\mathbf{R}_p|)Y_{lm}(\mathbf{r}-\mathbf{R}_p)$ in functions with center at $\mathbf{R}_n$ [see Eq. (A4)], Eq. (E1) takes the form

$$a_{lm}^n=\sum_{p\neq n}\sum_{l'm'}t_{l'}a_{l'm'}^p g_{lml'm'}^{(h)}(\mathbf{R}_p-\mathbf{R}_n). \tag{E5}$$

(The coefficients $g_{lml'm'}^{(h)}$ are given in Appendix A.) Moreover, using Bloch's theorem one can relate the coefficients a_{lm} of the different lattice sites

$$a_{lm}^p=e^{i\mathbf{k}\cdot(\mathbf{R}_p-\mathbf{R}_n)}a_{lm}^n. \tag{E6}$$

Substituting Eq. (E6) into Eq. (E5), we obtain

$$\sum_{l'm'}\left[\sum_{p\neq n} e^{i\mathbf{k}\cdot(\mathbf{R}_p-\mathbf{R}_n)} g^{(h)}_{lml'm'}(\mathbf{R}_p-\mathbf{R}_n) - (t_{l'}^{-1})\,\delta_{ll'}\,\delta_{mm'}\right] a^n_{l'm'}=0, \tag{E7}$$

which can be rewritten as

$$\sum_{l'm'}\left\{-ik_o\left[\sum_{\mathbf{R}_j\neq 0} e^{i\mathbf{k}\cdot\mathbf{R}_j} g^{(h)}_{lml'm'}(\mathbf{R}_j)+1\right] - k_o\,\mathrm{Im}(t_{l'}^{-1})\,\delta_{ll'}\,\delta_{mm'}\right\} a_{l'm'}=0. \tag{E8}$$

It is easy, using the formulas of the Appendixes A and B, to show that Eq. (E8) is identical with the secular equation (13).

[1] E. N. Economou and A. Zdetsis, Phys. Rev. B **40**, 1334 (1989).
[2] M. M. Sigalas and E. N. Economou, J. Sound Vib. **158**, 377 (1992).
[3] M. M. Sigalas and E. N. Economou, Solid State Commun. **86**, 141 (1993).
[4] E. N. Economou and M. M. Sigalas, in *Photonic Band Gaps and Localization*, edited by C. M. Soukoulis (Plenum, New York, 1993), pp. 317–338.
[5] E. N. Economou and M. M. Sigalas, J. Acoust. Soc. Am. **95**, 1734 (1994).
[6] J. O. Vasseur, B. Djafari-Rouhani, L. Dobrzynski, M. S. Kushwaha, and P. Halevi, J. Phys.: Condens. Matter **6**, 8759 (1994).
[7] M. S. Kushwaha, P. Halevi, G. Martinez, L. Dobrzynski, and B. Djafari-Rouhani, Phys. Rev. B **49**, 2313 (1994).
[8] J. V. Sánchez-Pérez, D. Caballero, R. Mártinez-Sala, C. Rubio, J. Sánchez-Dehesa, F. Meseguer, J. Llinares, and F. Gálvez, Phys. Rev. Lett. **80**, 5325 (1998).
[9] M. Kafesaki, M. M. Sigalas, and E. N. Economou, Solid State Commun. **96**, 285 (1995).
[10] M. Kafesaki, E. N. Economou, and M. M. Sigalas, in *Photonic Band Gap Materials*, edited by C. M. Soukoulis (Kluwer Academic, Dordrecht, 1996), pp. 143–164.
[11] M. S. Kushwaha, B. Djafari-Rouhani, L. Dobrzynski, and J. O. Vasseur, Eur. Phys. J. B **3**, 155 (1998).
[12] M. M. Sigalas and E. N. Economou, Europhys. Lett. **36**, 241 (1996).
[13] R. Mártinez-Sala, J. Sancho, J. V. Sánchez, V. Gomez, J. Llinres, and F. Meseguer, Nature (London) **378**, 241 (1995).
[14] F. R. Montero de Espinosa, E. Jiménez, and M. Torres, Phys. Rev. Lett. **80**, 1208 (1998).
[15] M. Torres, F. R. Montero de Espinosa, D. García-Pablos, and N. García, Phys. Rev. Lett. **82**, 3054 (1999).
[16] J. Korringa, Physica (Amsterdam) **XIII**, 392 (1947).
[17] W. Kohn and N. Rostoker, Phys. Rev. **94**, 1111 (1951).
[18] F. S. Ham and B. Segall, Phys. Rev. **124**, 1786 (1961).
[19] B. Segall and F. S. Ham, *Methods in Computational Physics* (Academic Press, London, 1968), Vol. 8, pp. 251–293.
[20] N. W. Ashcroft and D. N. Mermin, *Solid State Physics* (Holt, Rinehart and Winston, New York, 1976).
[21] Xindong Wang, X.-G. Zhang, Qingliang Yu, and B. N. Harmon, Phys. Rev. B **47**, 4161 (1993).
[22] Alexander Moroz, Phys. Rev. B **51**, 2068 (1995).
[23] Zhao-Qing Zhang and Lie-Ming Li, Phys. Rev. B **58**, 9587 (1998).
[24] M. Kafesaki and E. N. Economou, Phys. Rev. B **52**, 13 317 (1995).
[25] A. Klironomos and E. N. Economou, Solid State Commun. **105**, 324 (1998).
[26] N. Einspruch and R. Truell, J. Appl. Phys. **31**, 806 (1960).
[27] E. N. Economou, *Green's Functions in Quantum Physics* (Springer-Verlag, Berlin, 1983).
[28] A. R. Edmonds, *Angular Momentum in Quantum Mechanics* (Princeton University Press, Princeton, NJ, 1974).
[29] P. Ewald, Ann. Phys. (Leipzig) **64**, 253 (1921).